Bifurcation and chaos analysis of a nonlinear electromechanical coupling relative rotation system*

Liu Shuang(刘 爽)[a)b)], Zhao Shuang-Shuang(赵双双)[a)], Sun Bao-Ping(孙宝平)[a)], and Zhang Wen-Ming(张文明)[a)b)†]

[a)] *Key Laboratory of Industrial Computer Control Engineering of Hebei Province, Yanshan University, Qinhuangdao* 066004, *China*
[b)] *National Engineering Research Center for Equipment and Technology of Cold Strip Rolling, Yanshan University, Qinhuangdao* 066004, *China*

(Received 16 January 2014; revised manuscript received 25 February 2014; published online 16 July 2014)

Hopf bifurcation and chaos of a nonlinear electromechanical coupling relative rotation system are studied in this paper. Considering the energy in air-gap field of AC motor, the dynamical equation of nonlinear electromechanical coupling relative rotation system is deduced by using the dissipation Lagrange equation. Choosing the electromagnetic stiffness as a bifurcation parameter, the necessary and sufficient conditions of Hopf bifurcation are given, and the bifurcation characteristics are studied. The mechanism and conditions of system parameters for chaotic motions are investigated rigorously based on the Silnikov method, and the homoclinic orbit is found by using the undetermined coefficient method. Therefore, Smale horseshoe chaos occurs when electromagnetic stiffness changes. Numerical simulations are also given, which confirm the analytical results.

Keywords: relative rotation, electromechanical coupling, Hopf bifurcation, chaos

PACS: 45.20.dc, 05.45.−a **DOI:** 10.1088/1674-1056/23/9/094501

1. Introduction

Relative rotation system is a widespread power transmission system in project. Since the theory of rotational relativistic mechanics was first established by Carmeli in 1985.[1,2] Luo set up the theory of relativistic analytical mechanics of the rotational systems in 1996,[3,4] then rotational relativistic system has been an active research topic. Various nonlinear factors are contained in relative rotation system, which lead to the system complex dynamic behaviors such as bifurcation and chaos. Bifurcation and chaos are important parts of nonlinear scientific field.[5–8] They have achieved rapid development and extensive application in the fields of security communication,[9–11] signal processing,[12–14] and life science.[15–18]

Based on the relative rotation theory, a lot of research achievements about bifurcation and chaos of relative rotation system have been obtained in recent years. For two degrees of freedom, the Hopf bifurcation of relative rotation system was analyzed. The nonlinear and nonlinear time-delayed feedback control techniques were proposed to control the bifurcation points and the stability of periodic solutions.[19–21] The transfer concourse of primary resonance equation and topology structure of bifurcation function were obtained by singularity theory.[22] The bifurcation response equation of relative rotation system was deduced with the method of multiple scales, and the bifurcation and chaotic motions under combination resonance were investigated.[23,24] The chaotic behaviors of a relative rotation nonlinear dynamical system under parametric excitation and its control were studied in Refs. [25] and [26]. With research going deeper, the multi degrees of freedom coupling nonlinear relative rotation system has attracted more attention. The Hopf bifurcation of coupled system was analyzed under the conditions of primary resonance and internal resonance in Ref. [27]. The singularity stability of bifurcation function of principal resonance was investigated by singularity theory in Ref. [28]. A 4-dof torsional vibration model of nonlinear coupling relative rotation system was established, and the evolution process of period, period doubling and chaotic motions was studied.[29,30]

Ac motors have been widely used in relative rotation transmission system in recent years. Above papers better explained the mechanism of bifurcation and chaos from the viewpoints of mechanical parameters. However, the effect of electrical parameters were not taken into account. In this paper, the nonlinear electromechanical coupling model of relative rotation system is established considering the coupling effect of electrical parameters and mechanical parameters. The equilibrium and eignvalues of the equilibrium are analyzed. Using a combination of analytical and numerical methods, the mechanism and conditions of Hopf bifurcation and chaotic motions are investigated rigorously.

The rest of the paper is organized as follows. The nonlinear electromechanical coupling relative rotation system is presented in Section 2. The equilibrium and eigenvalues of

*Project supported by the National Natural Science Foundation of China (Grant No. 61104040) and the Natural Science Foundation of Hebei Province, China (Grant No. E2012203090).

†Corresponding author. E-mail: hudiezhaoshuang@163.com

© 2014 Chinese Physical Society and IOP Publishing Ltd

equilibrium are analyzed in Section 3. The Hopf bifurcation of nonlinear relative rotation system is analyzed in Section 4. Section 5 analyzes the chaotic behavior of relative rotation system based on the Silnikov method. Numerical simulations are performed in Sections 3 and 4, and some concluding remarks are provided in Section 6.

2. Electromechanical coupling relative rotation system

Considering a two masses relative rotation system driven by an ac motor, the total kinetic and potential energy of the system can be described as

$$T = \frac{1}{2}J_1\dot{\varphi}_1^2 + \frac{1}{2}J_2\dot{\varphi}_2^2, \tag{1}$$

$$V = \frac{1}{2}K(\varphi_1 - \varphi_2)^2. \tag{2}$$

The dissipation function is

$$F = \frac{1}{2}C(\dot{\varphi}_1 - \dot{\varphi}_2)^2 + \frac{1}{2}C_e\dot{\varphi}_1^2. \tag{3}$$

The air-gap magnetic field energy W_m between the stator and rotor is

$$W_m = \frac{RL}{2}\int_0^{2\pi} \Lambda(\alpha,t)F^2(\alpha,t)\,\mathrm{d}\alpha, \tag{4}$$

where J_i $(i=1,2)$ is the moment of inertia; φ_i $(i=1,2)$ and $\dot{\varphi}_i$ $(i=1,2)$ are angle of rotation and rotational speed, respectively; K is the torsional stiffness of drive shaft; C is the shafting damping coefficient; C_e is the electromagnetic damping coefficient (generated by the rotor damper bar); R is the average radius of the rotor; and L is the effective length of the rotor.

The air-gap permeance per unit area between the stator and rotor is

$$\begin{aligned}\Lambda(\alpha,t) = \Lambda_0\Big[1 &+ \frac{1}{2}\left(x'^2+y'^2\right) + x'\cos\alpha + y'\sin\alpha \\ &+ \frac{1}{2}\left(x'^2-y'^2\right)\cos 2\alpha + x'y'\sin 2\alpha\Big],\end{aligned} \tag{5}$$

where $\Lambda_0 = \mu_0/\sigma$, $\sigma = k_\mu\delta_0$, μ_0 is the air magnetic permeability, k_μ is the magnetic saturation, δ_0 is the equivalent air-gap, x' and y' are the synthetic eccentric, and α is the electric angle. By the geometrical dimensions of air gap, one may yield

$$x' = x_0 + x + \varepsilon_2\cos(\omega t + \varphi_1), \tag{6}$$

$$y' = y_0 + y + \varepsilon_2\sin(\omega t + \varphi_1), \tag{7}$$

where x_0 and y_0 are the static eccentric, ε_2 is the rotational eccentric, x and y are the amplitudes of transverse vibration. According to the electrical machine theory, the fundamental synthetic magneto motive force (mmf) between the stator and rator is

$$F(\alpha,t) = F_{sm}\cos(\omega t - \alpha) + F_{jm}\cos(\omega t + \varphi_1 - \alpha - \psi_1 - \psi_2), \tag{8}$$

where F_{sm} and F_{jm} are three phase fundamental synthetic mmf amplitudes of the stator and rotor, respectively. The phase angle of the rotor mmf lags behind the stator mmf $\psi_1 + \psi_2$. Substituting the Lagrangian function $L = T + W_m - V$ into dissipation Lagrange equation

$$\frac{\mathrm{d}}{\mathrm{d}t}\frac{\partial L}{\partial\dot{\varphi}_i} - \frac{\partial L}{\partial\varphi_i} + \frac{\partial F}{\partial\dot{\varphi}_i} = Q_i, \quad (i=1,2) \tag{9}$$

yields

$$\begin{cases} J_1\ddot{\varphi}_1 + K(\varphi_1-\varphi_2) + C(\dot{\varphi}_1-\dot{\varphi}_2) + C_e\dot{\varphi}_1 = M_e, \\ J_2\ddot{\varphi}_2 - K(\varphi_1-\varphi_2) - C(\dot{\varphi}_1-\dot{\varphi}_2) = M_d, \end{cases} \tag{10}$$

where M_e is the electromagnetic torque, and M_d is the load torque. In the case of no eccentricity, $M_e = \partial W_m/\partial\varphi_1 = k_0 + k_1\varphi_1 + k_2\varphi_1^2 + k_3\varphi_1^3$, where

$$\begin{aligned} k_0 &= -\pi RL\Lambda_0 F_{jm}F_{sm}\sin(\psi_1+\psi_2), \\ k_1 &= -\pi RL\Lambda_0 F_{jm}F_{sm}\cos(\psi_1+\psi_2), \\ k_2 &= -\frac{1}{2}\pi RL\Lambda_0 F_{jm}F_{sm}\sin(\psi_1+\psi_2), \\ k_3 &= \frac{1}{6}\pi RL\Lambda_0 F_{jm}F_{sm}\cos(\psi_1+\psi_2). \end{aligned}$$

It can be derived $k_1^2/a^2 + 4k_2^2/a^2 = 1$ $(a = -\pi RL\Lambda_0 F_{jm}F_{sm})$ and $k_3 = -k_1/6$ by the relationship of the trigonometric function. Thus, the nonlinear electromechanical coupling dynamic equation of relative rotation system is

$$\begin{cases} J_1\ddot{\varphi}_1 + K(\varphi_1-\varphi_2) + C(\dot{\varphi}_1-\dot{\varphi}_2) + C_e\dot{\varphi}_1 \\ = k_0 + k_1\varphi_1 + k_2\varphi_1^2 + k_3\varphi_1^3, \\ J_2\ddot{\varphi}_2 - K(\varphi_1-\varphi_2) - C(\dot{\varphi}_1-\dot{\varphi}_2) = M_d, \end{cases} \tag{11}$$

where electromagnetic stiffness K_e is the coefficient of φ_1 and $K_e = k_1$. Equation (11) is rewritten as

$$\begin{cases} J_1\ddot{\varphi}_1 + K(\varphi_1-\varphi_2) + C(\dot{\varphi}_1-\dot{\varphi}_2) + C_e\dot{\varphi}_1 - K_e\varphi_1 \\ = k_0 + k_2\varphi_1^2 + k_3\varphi_1^3, \\ J_2\ddot{\varphi}_2 - K(\varphi_1-\varphi_2) - C(\dot{\varphi}_1-\dot{\varphi}_2) = M_d. \end{cases} \tag{12}$$

Equation (12) is the nonlinear dynamic equation of two masses relative rotation system considering both electrical parameters and mechanical parameters, which is the basis of dynamic behavior analysis of electromechanical coupling relative rotation system. In the process of motor running, K_e is influenced by the motor load, the power supply voltage, and the current. Complex dynamic behaviors may occur with the changeable K_e for electromechanical coupling system. K_e is selected as a major parameter to analyze the system dynamic characteristics in the following.

3. Equilibrium point analysis

Let

$$x_1=\varphi_1,\ x_2=\dot{\varphi}_1,\ x_3=\varphi_2,\ x_4=\dot{\varphi}_2,\ a_1=\frac{K_e-K}{J_1},$$
$$b_1=-\frac{C+C_e}{J_1},\ c_1=\frac{K}{J_1},\ d_1=\frac{C}{J_1},\ l_1=\frac{k_2}{J_1},\ l_2=\frac{k_3}{J_1},$$
$$a_2=\frac{K}{J_2},\ b_2=\frac{C}{J_2},\ c_2=-\frac{K}{J_2},\ \text{and}\ d_2=-\frac{C}{J_2}.$$

Then system (12) can be expressed as

$$\dot{x}=f(x,K_e). \tag{13}$$

The equilibrium points of system (13) can be transferred into the origin of coordinates by a simple linear transformation, and it has universal significance to study the dynamic characteristics of system equilibrium point at the origin. Considering the equilibrium point at the origin of coordinates, equation (12) can be reduced order for first-order equation as follows:

$$\begin{cases}\dot{x}_1=x_2,\\ \dot{x}_2=a_1x_1+b_1x_2+c_1x_3+d_1x_4+l_1x_1^2+l_2x_1^3,\\ \dot{x}_3=x_4,\\ \dot{x}_4=a_2x_1+b_2x_2+c_2x_3+d_2x_4.\end{cases} \tag{14}$$

The Jacobian matrix of system (14) at $x_0=(0,0,0,0)$ can be expressed as

$$\boldsymbol{A}(x_0,K_e)=\begin{pmatrix}0&1&0&0\\ a_1&b_1&c_1&d_1\\ 0&0&0&1\\ a_2&b_2&c_2&d_2\end{pmatrix}. \tag{15}$$

The characteristic equation is

$$\lambda^4+p_1\lambda^3+p_2\lambda^2+p_3\lambda+p_4=0, \tag{16}$$

where $p_1=-d_2-b_1$, $p_2=-c_2+b_1d_2-b_2d_1-a_1$, $p_3=b_1c_2-b_2c_1+a_1d_2-a_2d_1$, and $p_4=a_1c_2-a_2c_1$.

It is not difficult to verify. Equation (16) is equivalent to

$$\lambda^2+\frac{P_1\pm\sqrt{8r_0+P_1^2-4P_2}}{2}\lambda+\left(r_0\pm\frac{P_1r_0-P_3}{\sqrt{8r_0+P_1^2-4P_2}}\right)=0, \tag{17}$$

where

$$r_0=\frac{P_2}{6}+\sqrt[3]{-\frac{q}{2}+\sqrt{\left(\frac{q}{2}\right)^2+\left(\frac{p}{3}\right)^3}}+\sqrt[3]{-\frac{q}{2}-\sqrt{\left(\frac{q}{2}\right)^2+\left(\frac{p}{3}\right)^3}},$$
$$p=\frac{p_1p_3-4p_4}{4}-\frac{p_2^2}{12},$$
$$q=\frac{p_1p_2p_3+8p_2p_4-3p_1^2p_4-3p_3^2}{24}+\frac{p_2^2}{54}.$$

Moreover, let

$$m_1=\frac{p_1+\sqrt{8r_0+p_1^2-4p_2}}{2},$$
$$n_1=r_0+\frac{P_1r_0-P_3}{\sqrt{8r_0+P_1^2-4P_2}},\ \Delta_1=m_1^2-4n_1,$$
$$m_2=\frac{p_1-\sqrt{8r_0+p_1^2-4p_2}}{2},$$
$$n_2=r_0-\frac{P_1r_0-P_3}{\sqrt{8r_0+P_1^2-4P_2}},\ \Delta_2=m_2^2-4n_2.$$

Therefore, equation (17) can be written as two equations

$$\lambda^2+m_1\lambda+n_1=0, \tag{18}$$

and

$$\lambda^2+m_2\lambda+n_2=0. \tag{19}$$

When K_e changes, there are two important situations for the eignvalues of Eq. (16).

Situation 1 When $\Delta_1<0$, $m_1>0$, $m_2=0$, and $n_2>0$, equation (18) has a pair of conjugate complex roots with negative real parts, and equation (19) has a pair of pure imaginary roots. When $m_1=0$, $n_1>0$, $\Delta_2<0$, and $m_2>0$, equation (18) has a pair of pure imaginary roots, and equation (19) has a pair of conjugate complex roots with negative real parts. In a word, the above two conditions all show that the characteristic equation (16) has a pair of pure imaginary roots and a pair of conjugate complex roots with negative real parts.

Situation 2 When $n_1<0$, $\Delta_2<0$, and $m_2>0$, equation (18) has a pair of conjugate complex roots with negative real parts, and equation (19) has two real roots of opposite sign. When $\Delta_1<0$, $m_1>0$, and $n_2<0$, equation (18) has two real roots of opposite sign, and equation (19) has a pair of conjugate complex roots with negative real parts. In a word, the above two conditions all show that the characteristic equation (16) has a pair of conjugate complex roots with negative real parts and two real roots of opposite sign.

In both situations, complicated dynamic behaviors may occur. Without loss of generality, we only consider $\Delta_1<0$, $m_1>0$, $m_2=0$, $n_2>0$, and $n_1<0$, $\Delta_2<0$, $m_2>0$. The discussion on the other two kinds of conditions are similar to these two.

4. Hopf bifurcation analysis

When the conditions in Situation 1 are satisfied, characteristic equation (16) has a pair of pure imaginary roots and a pair of conjugate complex roots with negative real parts. Hopf bifurcation may occur.

Let

$$\Delta_1'=p_1,\ \Delta_2'=\begin{vmatrix}p_1&p_0\\ p_3&p_2\end{vmatrix},\ \Delta_3'=\begin{vmatrix}p_1&1&0\\ p_3&p_2&p_1\\ 0&p_4&p_3\end{vmatrix}.$$

Δ_i' is Hurwitz determinant. Selecting $K_e = K_e^*$ as a Hopf bifurcation point, the conditions of Hopf bifurcation are

$$\begin{cases} p_i(K_e^*) > 0, \ \ i = (1,2,3,4), \\ \Delta_i'(K_e^*) > 0, \ \ i = (1,2), \\ \Delta_i'(K_e^*) = 0, \\ \dfrac{\mathrm{d}(\Delta_3'(K_e))}{\mathrm{d}K_e}\Big|_{K_e=K_e^*} \neq 0. \end{cases} \tag{20}$$

Take $b_1 = -0.2$, $c_1 = 1$, $d_1 = 0.4$, $a_2 = 1$, $b_2 = 0.4$, $c_2 = -1$, $d_2 = -0.1$, $l_1 = 0.5$, and $l_2 = -0.2$. Hopf bifurcation occurs when $K_e^* = -1.1582$, and $m_1 = 0.6 > 0$, $\Delta_1 = -8.4 < 0$, $m_2 = 0$, $n_2 = 0.43 > 0$ at this time, which satisfy the conditions in Situation 1.

Suppose that the pure imaginary roots are $\pm\omega_0 \mathrm{i}$, $\boldsymbol{U}$ and $\boldsymbol{W}$ are left and right normalized characteristic vectors of $\omega_0 \mathrm{i}$, respectively.

$$\boldsymbol{U}\boldsymbol{A} = \omega_0 \mathrm{i}\boldsymbol{U}, \ \ \boldsymbol{A}\boldsymbol{W} = \omega_0 \mathrm{i}\boldsymbol{W}, \ \ \boldsymbol{U}\boldsymbol{W} = 1. \tag{21}$$

Let

$$\begin{aligned} \rho \ = \ & \mathrm{Re}\big(-\boldsymbol{U}f_{xxx}\boldsymbol{W}\boldsymbol{W}\boldsymbol{W}^* + 2\boldsymbol{U}f_{xx}\boldsymbol{W}\boldsymbol{A}^{-1}(0)f_{xx}\boldsymbol{W}\boldsymbol{W}^* \\ & + \boldsymbol{U}f_{xx}\boldsymbol{W}^* \times [\boldsymbol{A}(0) - 2\mathrm{i}\omega_0\boldsymbol{I}]^{-1} f_{xx}\boldsymbol{W}\boldsymbol{W}\big), \end{aligned}$$

where $\boldsymbol{W}^*$ is conjugate complex of $\boldsymbol{W}$.

$$\boldsymbol{A}(0) = \boldsymbol{A}(x_0, K_e)|_{K_e=K_e^*}.$$

$$f_{xxx}\boldsymbol{W}\boldsymbol{W}\boldsymbol{W}^* = \frac{\partial}{\partial x}\left(\left(\frac{\partial}{\partial x}\left(\left(\frac{\partial f(x,K_e)}{\partial y}\right)\times \boldsymbol{W}\right)\boldsymbol{W}\right)\boldsymbol{W}^*\right)\Big|_{K_e=K_e^*, x=x_0}.$$

The stability of bifurcating periodic solutions is decided by the positive or negative of ρ. It obtained by calculation $\rho = 0.0051 > 0$, bifurcating periodic solutions are asymptotical stable, and limit cycles are stable. The results show that it is a supercritical bifurcation point. For supercritical bifurcation, when $K_e = -1.85 < K_e^*$, equilibrium point is asymptotically stable (see Fig. 1); when $K_e = -1.15 > K_e^*$, equilibrium point of the system is unstable and generate stable limit circles near it (see Fig. 2).

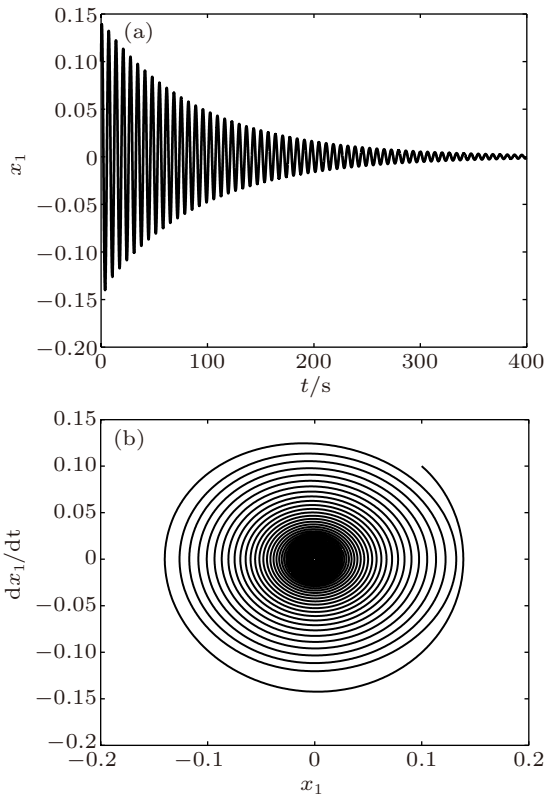


Fig. 1. Asymptotic stability of the equilibrium point: (a) time history and (b) phase diagram.

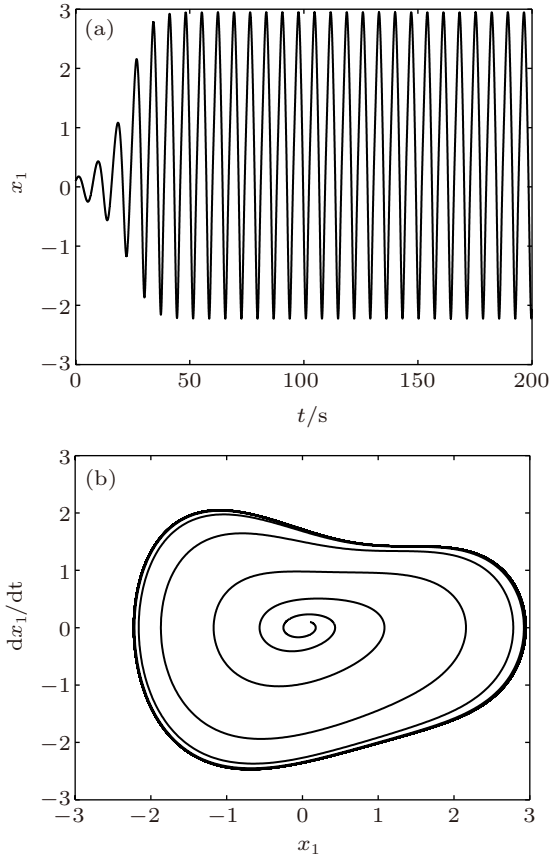


Fig. 2. Stable limit cycle: (a) time history and (b) phase diagram.

5. Silnikov chaos of the system

When the parameters satisfy the conditions in Situation 2 with the changeable K_e, x_0 is a saddle. Using the Silnikov method, considering the four-dimensional autonomous ordinary differential equation (14), we suppose that it has a homoclinic orbit connecting a hyperbolic equilibrium point to itself,

and the Jacobian matrix at the equilibrium point has the form (in appropriate local coordinates)

$$\begin{pmatrix} -\rho & -\omega & 0 & 0 \\ \omega & -\rho & 0 & 0 \\ 0 & 0 & -\lambda & 0 \\ 0 & 0 & 0 & \upsilon \end{pmatrix}, \tag{22}$$

where $\rho, \lambda > 0$, $\omega \neq 0$, $\upsilon > 0$ and satisfies $\upsilon > \rho > 0$, $\lambda \neq \upsilon$. Then the Smale horseshoe chaos occurs.

Using the undetermined coefficient method,[31,32] a homoclinic orbit connecting x_0 to itself will be found. In the case of $t > 0$, we assume that

$$\begin{pmatrix} x_1(t) \\ x_2(t) \\ x_3(t) \\ x_4(t) \end{pmatrix} = \begin{pmatrix} \sum_{k=1}^{\infty} e_k \mathrm{e}^{k\sigma t} \\ \sum_{k=1}^{\infty} f_k \mathrm{e}^{k\sigma t} \\ \sum_{k=1}^{\infty} g_k \mathrm{e}^{k\sigma t} \\ \sum_{k=1}^{\infty} h_k \mathrm{e}^{k\sigma t} \end{pmatrix}, \tag{23}$$

where e_k, f_k, g_k, and h_k are undetermined coefficients, and σ is a decaying exponent.

Substituting Eq. (23) into Eq. (14) and equating the coefficients of like powers of $\mathrm{e}^{k\sigma t}$, it yields a set of algebraic equations with the undetermined coefficients.

For $k = 1$, we have

$$(\sigma \boldsymbol{I} - \boldsymbol{A}(x_0)) \begin{pmatrix} e_1 \\ f_1 \\ g_1 \\ h_1 \end{pmatrix} = \begin{pmatrix} 0 \\ 0 \\ 0 \\ 0 \end{pmatrix}. \tag{24}$$

Assume $(e_1, f_1, g_1, h_1) \neq 0$, otherwise we can inductively conclude that $(e_k, f_k, g_k, h_k) = 0$ for all $k > 1$. e_1, f_1, g_1, h_1 can be determined with a free parameter ξ when $\det(\sigma \boldsymbol{I} - \boldsymbol{A}) = 0$. If x_0 is a saddle, there exists a unique negative σ such that $\det(\sigma \boldsymbol{I} - \boldsymbol{A}) = 0$. Meanwhile, the expressions of e_1, f_1, g_1, and h_1 in terms of parameter ξ can be obtained by Eq. (24).

For $k = 2$, we have

$$(2\sigma \boldsymbol{I} - \boldsymbol{A}(x_0)) \begin{pmatrix} e_2 \\ f_2 \\ g_2 \\ h_2 \end{pmatrix} = \begin{pmatrix} 0 \\ l_1 e_1^2 \\ 0 \\ 0 \end{pmatrix}. \tag{25}$$

Note that $\det(2\sigma \boldsymbol{I} - \boldsymbol{A}) \neq 0$, so e_2, f_2, g_2, and d_2 have been uniquely determined by Eq. (25).

Inductively, for $k > 3$, we have

$$(k\sigma \boldsymbol{I} - \boldsymbol{A}(x_0)) \begin{pmatrix} e_k \\ f_k \\ g_k \\ h_k \end{pmatrix} = \begin{pmatrix} 0 \\ l_1 \sum\limits_{i+j=k} e_i e_j + l_2 \sum\limits_{l+m+n=k} e_l e_m e_n \\ 0 \\ 0 \end{pmatrix}. \tag{26}$$

As a result of $\det(k\sigma \boldsymbol{I} - \boldsymbol{A}) \neq 0 (k > 1)$, so e_k, f_k, g_k, and h_k have been uniquely determined by Eq. (26). Therefore, for $t > 0$, $x_1(t)$, $x_2(t)$, $x_3(t)$, and $x_4(t)$ have been uniquely determined.

For the reverse time-asymptotic trajectories, we use the transformation $\tau = -t$ with $t > 0$. Then equation (14) becomes

$$\begin{pmatrix} \frac{\mathrm{d}x_1}{\mathrm{d}\tau} \\ \frac{\mathrm{d}x_2}{\mathrm{d}\tau} \\ \frac{\mathrm{d}x_3}{\mathrm{d}\tau} \\ \frac{\mathrm{d}x_4}{\mathrm{d}\tau} \end{pmatrix} = \begin{pmatrix} -x_2 \\ -a_1 x_1 - b_1 x_2 - c_2 x_3 - d_2 x_4 - l_1 x_1^2 - l_2 x_1^3 \\ -x_4 \\ -a_2 x_1 - b_2 x_2 - c_2 x_3 - d_2 x_4 \end{pmatrix}. \tag{27}$$

Completely similar to the case of $t > 0$, we assume that

$$\begin{pmatrix} x_1(t) \\ x_2(t) \\ x_3(t) \\ x_4(t) \end{pmatrix} = \begin{pmatrix} \sum_{k=1}^{\infty} e'_k \mathrm{e}^{-k\sigma'\tau} \\ \sum_{k=1}^{\infty} f'_k \mathrm{e}^{-k\sigma'\tau} \\ \sum_{k=1}^{\infty} g'_k \mathrm{e}^{-k\sigma'\tau} \\ \sum_{k=1}^{\infty} h'_k \mathrm{e}^{-k\sigma'\tau} \end{pmatrix}. \tag{28}$$

By comparing the coefficients of like powers of $\mathrm{e}^{-k\sigma'\tau}$, we obtain a set of algebraic equations with the undetermined coefficients e'_k, f'_k, g'_k, and h'_k and the decaying exponent σ'. For $k = 1$, we have

$$(-\sigma' \boldsymbol{I} - \boldsymbol{A}) \begin{pmatrix} e'_k \\ f'_k \\ g'_k \\ h'_k \end{pmatrix} = \begin{pmatrix} 0 \\ 0 \\ 0 \\ 0 \end{pmatrix}. \tag{29}$$

Therefore, $\sigma = \sigma'$, the other coefficients e'_k, f'_k, g'_k, h'_k can also be uniquely determined with a free parameter η. Let $\eta = \xi$, we have

$$\begin{aligned} e'_k(S, \sigma, \xi) &= e_k(S, -\sigma, \xi), \\ f'_k(S, \sigma, \xi) &= f_k(S, -\sigma, \xi), \\ g'_k(S, \sigma, \xi) &= g_k(S, -\sigma, \xi), \\ h'_k(S, \sigma, \xi) &= h_k(S, -\sigma, \xi), \end{aligned} \tag{30}$$

where $S = \{a_1, b_1, c_1, d_1, a_2, b_2, c_2, d_2\}$ is the set of system parameters, and the continuity of $x_1(t)$, $x_2(t)$, $x_3(t)$, and $x_4(t)$ will determine the value of ξ.

According to the above analysis, the expressions of the homoclinic orbit connecting the equilibrium point x_0 to that of system (14) are obtained as follows:

$$\begin{aligned} x_1(t) &= \begin{cases} \sum_{k=1}^{\infty} e_k(s, \sigma, \xi) \mathrm{e}^{k\sigma t} (t > 0), \\ \sum_{k=1}^{\infty} e_k(s, -\sigma, \xi) \mathrm{e}^{-k\sigma\tau} (t < 0); \end{cases} \\ x_2(t) &= \begin{cases} \sum_{k=1}^{\infty} f_k(s, \sigma, \xi) \mathrm{e}^{k\sigma t} (t > 0), \\ \sum_{k=1}^{\infty} f_k(s, -\sigma, \xi) \mathrm{e}^{-k\sigma\tau} (t < 0); \end{cases} \\ x_3(t) &= \begin{cases} \sum_{k=1}^{\infty} g_k(s, \sigma, \xi) \mathrm{e}^{k\sigma t} (t > 0), \\ \sum_{k=1}^{\infty} g_k(s, -\sigma, \xi) \mathrm{e}^{-k\sigma\tau} (t < 0); \end{cases} \\ x_4(t) &= \begin{cases} \sum_{k=1}^{\infty} h_k(s, \sigma, \xi) \mathrm{e}^{k\sigma t} (t > 0), \\ \sum_{k=1}^{\infty} h_k(s, -\sigma, \xi) \mathrm{e}^{-k\sigma\tau} (t < 0); \end{cases} \end{aligned} \tag{31}$$

where e_k, f_k, g_k, and h_k are given by Eqs. (24)–(26), σ by

$\det(\sigma \boldsymbol{I} - \boldsymbol{A}) = 0$, and ξ by

$$\sum_{k=1}^{\infty} e_k(s, \sigma, \xi) = \sum_{k=1}^{\infty} e_k(s, -\sigma, \xi). \tag{32}$$

The results are obtained according to the silnikov method.

Theorem 1 If $n_1 < 0$, $\Delta_2 < 0$, $m_2 > 0$, $\sqrt{\Delta_1} > p_1$, and $m_1 \neq 0$, then system (14) has a homoclinic orbit joining the initial equilibrium point x_0 to itself with Eq. (31). The Smale horseshoe chaos occurs.

From the expression of K_e, we know that K_e is decided by the value of F_{sm}, F_{jm}, and the phase difference $\psi_1 + \psi_2$. Three phase fundamental synthetic mmf amplitudes of the stator and rotor $F_{sm} = (3/2) \times 0.9 I_s \frac{W}{p} K_{d1} K_{p1}$ ($F_{jm} = (3/2) \times 0.9 I_j \frac{W}{p} K_{d1} K_{p1}$), where W, p, K_{d1}, and K_{p1} are all constant. Suppose that the $\psi_1 + \psi_2$ is a fixed value, K_e can be changed by adjusting the stator current I_s and the rotor current I_j. System parameters can be taken as $b_1 = -0.22$, $c_1 = 0.11$, $d_1 = 0.05$, $a_2 = -10.28$, $b_2 = 0.05$, $c_2 = -0.11$, $d_2 = -0.05$. Let K_e change in a wide range. The bifurcation diagram and the maximum Lyapunov exponent of relative rotation system (14) are shown in Figs. 3 and 4. It can be seen that with the increase in K_e, periodic motion and chaotic motion appear alternately. Phase trajectory, Poincare map, and power spectrum are shown in Fig. 5 under different K_e. When $K_e = 3$, system response is a stable periodic motion. It can be seen from panels (a1)–(a3) in Fig. 5 that the phase trajectory for closed curves, the poincare map for a finite number of fixed points, and the power spectrum are three obvious peak values. When $K_e = 7$, system (14) has a homoclinic orbit joining the initial equilibrium point to itself, and satisfy the parameter conditions in Theorem 1. The system is chaotic. From Fig. 4, the maximum Lyapunov exponent is greater than zero under K_e=7, it can be convince of occurrence of chaotic motion. We can also see that the phase trajectory repeatedly winding in enclosed area but not closed, Poincare section has a obvious fractal structure, and power spectrum is continuous (see panels (b1)–(b3) in Fig. 5).

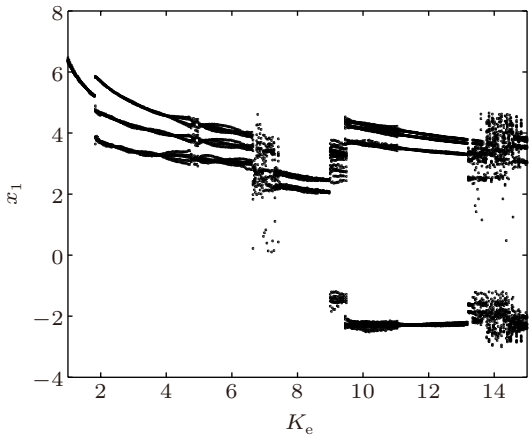


Fig. 3. Bifurcation diagram of system (14): K_e is varied from 1 to 15.

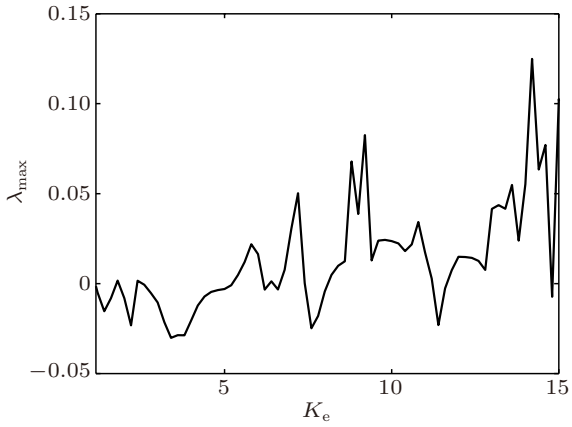


Fig. 4. The maximum Lyapunov exponent corresponding to Fig. 1.

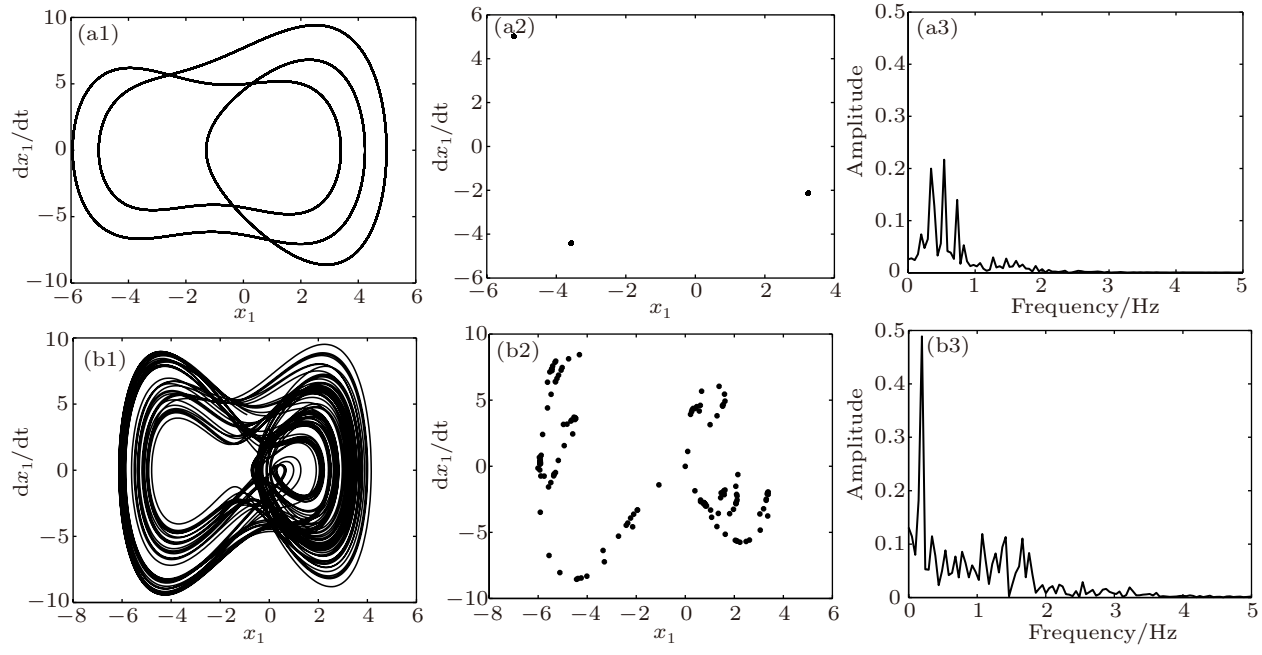


Fig. 5. Phase trajectory (a1, b1), Poincare map (a2, b2), and power spectrum (a3, b3) for different K_e. (a1)–(a3) $K_e = 3$; (b1)–(b3) $K_e = 7$.

6. Conclusion

In this paper, the dynamic equation of nonlinear reltive rotation system with electromagnetic stiffness and electromagnetic damping is deduced according to the Lagrange–Maxwell equation. The Hopf bifurcation and chaotic motions of the system are studied under different electromagnetic stiffness. Numerical simulation results show that bifurcation and chaos can be controlled by reasonable selection on electromagnetic stiffness. Electromagnetic stiffness is influenced by the voltage and current of the motor in engineering. The system bifurcation and chaotic motions can be controlled effectively by adjusting voltage and current. These results have an important theoretical significance on reducing the vibration of electromechanical coupling relative rotation system. In addition, the research in our paper provides a reference for further studying complex nonlinear dynamics behaviors of large rotary machinery.

References

[1] Carmeli M 1985 *Found. Phys.* **15** 175
[2] Carmeli M 1986 *Int. J. Theor. Phys.* **25** 89
[3] Luo S K 1996 *J. Beijing Inst. Technol.* **16** 154 (in Chinese)
[4] Luo S K 1998 *Appl. Math. Mech.* **19** 45
[5] Wang X Y and Wang M J 2008 *Physica A* **387** 3751
[6] Li N, Sun H Y and Zhang Q L 2012 *Chin. Phys. B* **21** 010503
[7] Ma C and Wang X Y 2012 *Commun. Nonlinear Sci. Numer. Simulat.* **17** 721
[8] Zhang L S, Cai L and Feng C W 2010 *Acta Electron. Sin.* **38** 1 (in Chinese)
[9] Wang X Y and Wang L L 2011 *Chin. Phys. B* **20** 050509
[10] Wu G and Cai L 2010 *Chin. J. Sci. Instrument* **31** 454 (in Chinese)
[11] Bao H M and Zhu Y S 2009 *Acta Electron. Sin.* **37** 1222 (in Chinese)
[12] Wang X Y, Liang Q Y and Meng J 2008 *Int. J. Mod. Phys. C* **19** 1389
[13] Wang X Y and Liang Q Y 2008 *Commun. Nonlinear Sci. Numer. Simul.* **13** 913
[14] Chen J S, Zeng Y C, Chen S B and Li J B 2011 *Chin. J. Sci. Instrument* **32** 1710 (in Chinese)
[15] Wang X Y, Luo C and Meng J 2009 *Appl. Math. Comput.* **207** 63
[16] Wang X Y and Luo C 2006 *Appl. Math. Comput.* **183** 30
[17] Luo C W, Wang C C and Wei J J 2009 *Chaos Soliton. Fract.* **39** 1831
[18] Luo Z Z, Li Y F, Meng M and Sun Y 2011 *Chin. J. Sci. Instrument* **32** 33 (in Chinese)
[19] Liu S, Liu B and Shi P M 2009 *Acta Phys. Sin.* **58** 4383 (in Chinese)
[20] Liu S, Liu B, Zhang Y K and Wen Y 2010 *Acta Phys. Sin.* **59** 38 (in Chinese)
[21] Shi P M, Li J Z, Liu B and Han D Y 2011 *Acta Phys. Sin.* **60** 094501 (in Chinese)
[22] Liu H R, Zhu Z L and Shi P M 2010 *Acta Phys. Sin.* **59** 6770 (in Chinese)
[23] Meng Z, Fu L Y and Song M H 2013 *Acta Phys. Sin.* **62** 054501 (in Chinese)
[24] Li H B, Wang B H, Zhang Z Q, Liu S and Li Y S 2012 *Acta Phys. Sin.* **61** 094501 (in Chinese)
[25] Shi P M, Liu B and Hou D X 2009 *Chin. J. Mechan. Eng.* **22** 132
[26] Shi P M, Han D Y and Liu B 2010 *Chin. Phys. B* **19** 090306
[27] Liu S, Liu H R, Wen Y and Liu B 2010 *Acta Phys. Sin.* **59** 5223 (in Chinese)
[28] Shi P M, Liu B and Jiang J S 2009 *Acta Phys. Sin.* **58** 2147 (in Chinese)
[29] Meng L Q, Wu H L, Wang J X and Lei M J 2009 *Journal of Central South University: Sci. Technol.* **40** 1228 (in Chinese)
[30] Meng L Q, Wang J X, Wu H L and Lei M J 2009 *Journal of South China University of Technology: Natural Science Edition* **37** 25 (in Chinese)
[31] Qi G Y, Chen G R and Zhang Y H 2008 *Chaos Soliton. Fract.* **37** 409
[32] Zhou T and Tang Y 2004 *Int. J. Bifurc. Chaos* **14** 3167